

# Structural Changes in Tribo-Stressed Zinc Polyphosphates

Sophia Berkani · Fabrice Dassenoy · Clotilde Minfray ·  
Jean-Michel Martin · Herve Cardon · Gilles Montagnac ·  
Bruno Reynard

Received: 3 April 2013 / Accepted: 9 July 2013 / Published online: 19 July 2013  
© Springer Science+Business Media New York 2013

**Abstract** The influences of pressure, shear stress and temperature on the structure of zinc orthophosphate and zinc metaphosphate was investigated. Tribological tests were performed to study the combined effect of pressure and shear stress at two temperatures. Friction tests were carried out in the boundary lubrication regime from dispersions of zinc polyphosphates in base oil. The effects of pressure alone were investigated using a diamond anvil cell in order to separate it from those of shearing. Raman spectroscopy was used to follow in situ or ex situ the structural changes of the zinc polyphosphate powders and the tribo-stressed areas. Tribofilms obtained with both polyphosphates display a partial and full depolymerization of the zinc metaphosphate at ambient and high (120 °C) temperature, respectively. The large stress and strain conditions of the tribological tests are necessary to induce a tribochemical reaction between zinc metaphosphate and iron oxide leading to a depolymerization of the phosphate in the tribofilm. The tribochemical reaction and antiwear tribofilm formation are significantly enhanced by the modest temperature increase from ambient to 120 °C. Pressure alone induces only disordering in the structure of zinc polyphosphates, with only minor changes of the chain length in phosphates and does not contribute significantly to the observed structural changes in tribofilms.

**Keywords** Antiwear additives · Tribochemistry · Boundary lubrication · Zinc polyphosphates · Raman

## 1 Introduction

Zinc dialkyldithiophosphate (ZDDP) has been recognized as a multifunctional additive in engine oils for over 70 years. It is widely used in formulating lubricants to enhance their antioxidant, antiwear and extreme pressure properties. When tribo-stressed in a lubricated tribological contact under severe friction conditions, the ZDDP molecule is thermally degraded and eventually forms a thin antiwear solid-like protective film (called a tribofilm) about one hundred nanometers thick on the metal rubbing surfaces. This film is known to protect the surfaces from adhesion and abrasion [1]. It presents a heterogeneous morphology, including pads and valleys of irregular sizes [1]. Chemical composition varies gradually from the top of the film to the substrate [2]. It is well established that the tribofilm is mostly composed of amorphous zinc/iron polyphosphates with variable chain lengths, with inclusions of ZnS and FeS [2–4]. Mostly orthophosphates (with mixed Zn and Fe) are found near the tribofilm contact with the steel surface while polyphosphates (mostly zinc metaphosphate composition) are located at the top surface of the tribofilm.

Several mechanisms have been proposed in the literature to explain the formation, the antiwear action of ZDDP tribofilm [3–11], as well as the formation of the gradient of phosphate chain length (or polymerization) in the film thickness. Martin [12] proposed a mechanism derived from the Chemical Hardness model of Pearson [13]. Firstly, the ZDDP undergoes a thermo-oxidative decomposition in the bulk of the lubricant. At temperatures above 100 °C, a

S. Berkani · F. Dassenoy (✉) · C. Minfray · J.-M. Martin  
LTDS, Ecole Centrale de Lyon, UMR 5513, 36 Avenue Guy de  
Collongue, 69134 Ecully, France  
e-mail: fabrice.dassenoy@ec-lyon.fr

S. Berkani · H. Cardon · G. Montagnac · B. Reynard  
LGL, Ecole Normale Supérieure de Lyon, Université Claude  
Bernard Lyon1, CNRS, 15 Parvis René Descartes, 69364 Lyon,  
France

thermal film of zinc long-chain poly(thio)phosphate forms on the metal surface by static adsorption, with a depletion of sulfur with respect to the ZDDP stoichiometry. Secondly, under friction, an acid–base reaction occurs between the zinc polyphosphate (thermal film) and the native iron oxide of the steel substrate, ensuring good adhesion of the film on the substrate [12]. The reaction between the zinc metaphosphate and the iron oxide particles leads to the depolymerization of the polyphosphate chains near the metallic surface, explaining well the gradient of phosphate chain in the tribofilm. In subsequent steps of the reaction, if metallic wear debris from other parts of the system is coming in the contact area, digestion of the iron oxide by zinc polyphosphates is possible and reduces abrasive wear. As thermal degradation continues during the test, the composite structure of the tribofilm is created.

Nicholls et al. [4] suggested that the chain length of phosphate may also vary with the pressure applied on the tribofilm. According to this hypothesis, pressure alone could induce a cross-linking of the phosphate chains, leading to the presence of longer zinc polyphosphate chains at the surface of the tribofilm than in direct contact of the steel surface. However, this author does not consider the role of iron in the process. The effects of pressure alone on the tribofilm were studied by first-principles molecular dynamics simulations of compression/decompression phases, under hydrostatic conditions, of zinc polyphosphates used as model materials [14]. A change in the coordination of zinc atom with pressure was predicted which would lead to a highly interconnected network of zinc phosphate chains.

The influence of pressure alone on the structure of zinc polyphosphate compounds of different chain lengths was recently investigated using DAC that provides a quasi-hydrostatic environment coupled to different analytical in situ methods (Raman spectroscopy, EXAFS, XRD) [15–18]. Gauvin et al. [15] evidenced structural changes in phosphates by Raman spectroscopy (mainly amorphization) at very high pressures (>20 GPa), but no effect was observed on the degree of polymerization of the zinc phosphate compounds. Further experiments on crystalline zinc orthophosphate confirmed these findings [18, 19].

The effect of tribological stress (shear and pressure) on these model materials was also investigated [17, 20]. Crobu et al. [20, 21] carried out tribological tests at ambient temperature on amorphous glasses of zinc metaphosphate. A tribofilm was obtained and the postmortem analysis highlighted a depolymerization of the zinc metaphosphate in agreement with the Chemical Hardness model. Iron oxide species were also found in the tribofilm.

In spite of these recent studies, the origin of the gradient of phosphate chain length in the ZDDP tribofilm is still unclear. We test here the hypothesis that metaphosphates

are depolymerized under the combined action of shear, pressure and temperature in the tribological contact. We compare the behavior of two model compounds: a zinc orthophosphate (isolated tetrahedra) and a zinc metaphosphate (infinite chains). Their structural changes were monitored using Raman spectroscopy under pure hydrostatic pressure for comparing with the combined effect of the pressure and shearing in tribological tests. The effects of temperature on the reactions were investigated by performing the tribological tests at ambient and elevated (120 °C) temperatures.

## 2 Experimental

### 2.1 Materials

A few micron-size commercial zinc orthophosphate powder [ $\text{Zn}_3(\text{PO}_4)_2$ , 99.99 %] provided by Alfa Aesar was used without further purification. Owing to their high hygroscopic properties, phosphates break down in the presence of atmospheric humidity. Thus, powders were heated to 520 °C during 24 h prior to analysis and stored in dry atmosphere. After this treatment, a pure white crystalline powder of zinc phosphate is obtained with the  $\alpha\text{-Zn}_3(\text{PO}_4)_2$  structure, in which tetrahedral phosphate  $\text{PO}_4$  monomers are linked to Zn cations through terminal oxygen atoms [16]. Zinc metaphosphate was supplied by Pr. Richard K. Brow from the University of Missouri-Rolla.

### 2.2 DAC Experiments

High-pressure experiments were performed on the crystalline phases. A diamond anvil cell (DAC) equipped with 500-micron culet diamond anvils was used. A few ruby chips were placed inside the gasket sample chamber as pressure calibrants. The sample chamber consists in a 500-micron hole drilled in a stainless-steel-preindented gasket. The pressure was determined from the well-known pressure shift of the R1 ruby fluorescence line (at  $5,029\text{ cm}^{-1}$  under ambient conditions) [22]. Raman spectra were recorded in the backscattered geometry with a Labram HR800 equipped with a notch filter and a  $1,800\text{ g mm}^{-1}$  monochromator which achieves a  $1\text{ cm}^{-1}$  resolution. Acquisition time was around 300 s. The 514.5-nm excitation wavelength is provided by a Ar+ laser. For this study, 280 mW were delivered by the laser yielding a few milliwatts on the sample. A microscope is combined to the spectrometer in order to deliver a few-micron-wide spot on the sample. Raman experiments were performed in an air-conditioned room at 20 °C with a relative humidity of 30–40 RH.

### 2.3 Tribological Tests

Zinc polyphosphate powders were added at a 5 wt% concentration to a polyalphaolefin 6 base oil. Sliding tests were performed using a homemade reciprocating sphere-on-flat tribometer. The employed disks and balls had a roughness inferior to 20 nm (Ra). All specimens are made of AISI2100 steel (100C6) hardened to 800HV. The balls used had a diameter of 12.7 mm. Before the tribological tests, both sliding counterfaces (balls and disks) were cleaned in ultrasonic bath for 10 min in dichloromethane, acetone, isopropanol and heptane and wiped with a cleaning tissue. A 25 N normal load was applied, yielding a maximum Hertzian contact pressure of 1.16 GPa. The tests were performed in ambient atmosphere (35–45 RH) and at two temperatures (ambient temperature and 120 °C). The track length was initially set to 2 mm and the sliding speed to 2.5 mm s<sup>-1</sup>. All tests were carried out in a lubricated environment. At the end of each test, disks and balls were cleaned in ultrasonic bath for 10 min in heptane.

## 3 Results

### 3.1 Raman Spectroscopy of Zinc Polyphosphates at Atmospheric Pressure

The two zinc polyphosphates were characterized by Raman spectroscopy. Vibration bands of phosphate bonds lie between 400 and 1,400 cm<sup>-1</sup> and can be divided into three sub-regions: the region of low frequencies (<600 cm<sup>-1</sup>), corresponding to the bending modes of the tetrahedra, the high-frequency region (≥800 cm<sup>-1</sup>), where the stretching modes of P–O bonds can be observed, and an intermediate region between 600 and 800 cm<sup>-1</sup> corresponding to the stretching vibration modes of the P–O–P bonds.

#### 3.1.1 Ambient Temperature

In zinc orthophosphate (Fig. 1a), the observed spectrum is in agreement with previous studies [18, 23]. Above 800 cm<sup>-1</sup>, three high-intensity bands at 965.5, 1,007.8 and 1,047.7 cm<sup>-1</sup> can be observed together with a doublet at 1,157.2 and 1,176.1 cm<sup>-1</sup>, corresponding to the stretching vibration mode of symmetrical and antisymmetrical isolated phosphate ( $\nu_{P-O}$ ). The absence of bands in the range 600–800 cm<sup>-1</sup> confirms that the sample contains only zinc monophosphates [24]. A high-intensity band at 426 cm<sup>-1</sup> and four other bands of lower intensities at 448, 514, 553 and 594 cm<sup>-1</sup> can be observed in the low-frequency region (<600 cm<sup>-1</sup>). These bands are assigned to the bending vibrations of the phosphate tetrahedra ( $\delta_{P-O}$ ). The bands visible below 400 cm<sup>-1</sup> are lattice modes ( $\delta_{P-O}$ ).

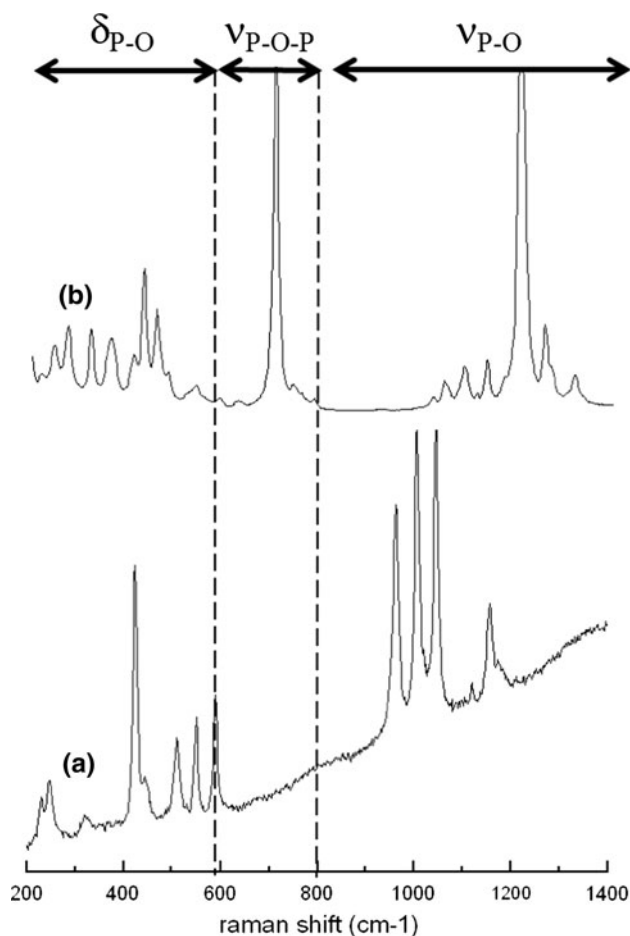


**Fig. 1** Raman spectra of zinc phosphates at atmospheric pressure and ambient temperature in the 200–1,400 cm<sup>-1</sup> range of: **a** pure crystalline orthophosphate ( $\alpha$ -Zn<sub>3</sub>(PO<sub>4</sub>)<sub>2</sub>), **b** pure crystalline zinc metaphosphate ( $\beta$ -Zn(PO<sub>3</sub>)<sub>2</sub>)

In zinc metaphosphate (Fig. 1b), two strong intensity bands are observed: one at 707.5 cm<sup>-1</sup> which is characteristic of the chains corresponds to the symmetric stretching vibration of the P–O–P bond ( $\nu_{P-O-P}$ ), and one at 1,211.9 cm<sup>-1</sup>, corresponding to the antisymmetric stretching vibration mode of P–O bonds ( $\nu_{P-O}$ ). Bending modes of the tetrahedra and lattice modes are observed in the low-frequency range (<600 cm<sup>-1</sup>).

#### 3.1.2 Melted Phosphates

In order to obtain the Raman spectra of the amorphous zinc polyphosphates compounds, the ortho- and metapolyphosphates were heated using a heating stage up to their liquid state (~1,000 °C) and analyzed at this temperature by Raman spectroscopy (Fig. 2). Spectra of the two zinc polyphosphates show much broader bands (increase in full width at half maximum or FWHM—see Table 1), reflecting both the effect of heating and the structural disorder

induced by melting of the two phosphates. Increasing temperature also results in a shift of the peaks to lower frequencies.

For zinc orthophosphate (Fig. 2a), the bands located at low frequencies become considerably broader. However, the deformation vibration bands of the phosphate tetrahedra ( $\delta_{\text{P-O}}$ ) at 417.7, 488.4, 545.9 and 579.3  $\text{cm}^{-1}$  are clearly observed. Above 800  $\text{cm}^{-1}$ , a single intense broad band at 966  $\text{cm}^{-1}$  is observed in place of the three most intense bands of the crystalline compound and corresponds to the symmetric stretching mode of isolated phosphates ( $\nu_{\text{P-O}}$ ). The peak observed at 1,070  $\text{cm}^{-1}$  corresponds to the antisymmetric stretching mode, and its presence indicates that the tetrahedra are still distorted from perfect  $T_d$  symmetry in the liquid. However, the absence of significant intensity in the 600–800  $\text{cm}^{-1}$  range (corresponding to the P–O–P bond) indicates little on the polymerization in the melt. The orthophosphate nature of the compound is thus largely preserved.

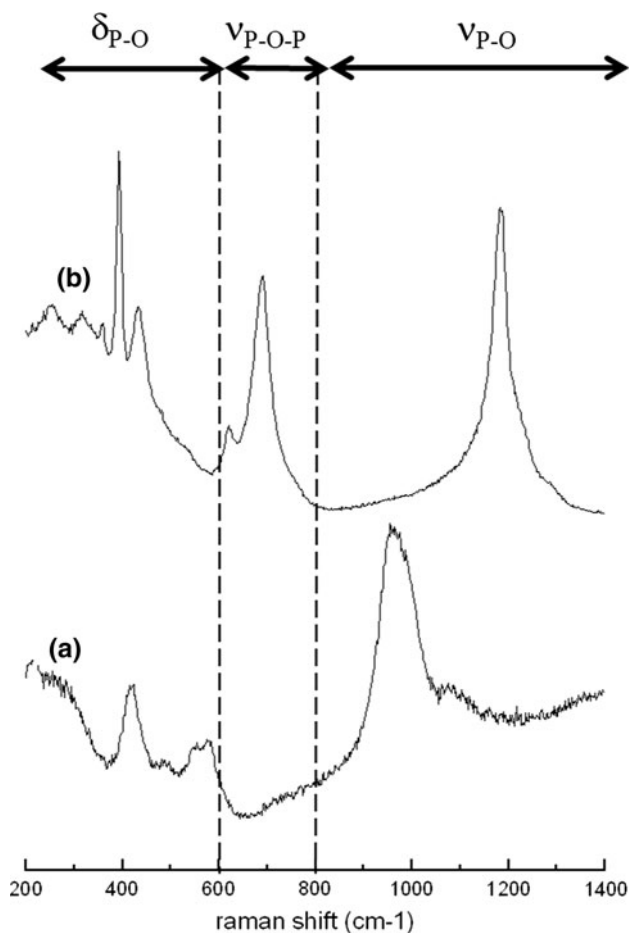


**Fig. 2** Raman spectra of zinc phosphates at 1,000 °C (liquid state) in the 200–1,400  $\text{cm}^{-1}$  range of: **a** zinc orthophosphate ( $\text{Zn}_3(\text{PO}_4)_2$ ), **b** zinc metaphosphate ( $\text{Zn}(\text{PO}_3)_2$ )

For zinc metaphosphate (Fig. 2b), the two most characteristic bands of the metaphosphate above 600  $\text{cm}^{-1}$  are much broader than those observed in the crystalline phase. The symmetric stretching vibration band ( $\nu_{\text{P-O-P}}$ ) occurs at 684  $\text{cm}^{-1}$ , and the band corresponding to the antisymmetric stretching vibration mode of the P–O bonds ( $\nu_{\text{P-O}}$ ) at 1,182  $\text{cm}^{-1}$ .

### 3.2 DAC Experiments: Behavior of Zinc Polyphosphates Under Pressure

Pressure was increased by steps to a maximum of 12 GPa corresponding to about ten times the highest estimates of pressure peaks in the tribological contact. Pressure was allowed to relax to a stable value prior to the acquisition of the Raman spectra at each step. Tests were performed at room temperature and reproduced three times.

#### 3.2.1 Zinc Orthophosphate

Figure 3 shows a series of Raman spectra recorded at different compression stages of crystalline zinc orthophosphate powder under pressures up to 12 GPa and after decompression at room temperature.

As pressure increases, the peaks of interest shift continuously to higher wavenumbers. This positive pressure-induced Raman shift is typical of bond compression. Above 1.3 GPa, the relative intensities of the peaks around 1,000  $\text{cm}^{-1}$  are strongly changed. While the relative intensity of the peak at 965  $\text{cm}^{-1}$  grows, the intensity of the other ones decreases. In addition, peaks broaden as pressure increases, indicating progressive disordering of the structure of the compound, which tends to become amorphous, as its spectrum is similar to that of the melt at high temperatures (Fig. 2a).

After decompression, the sample is irreversibly modified, yielding a spectrum similar to that of the orthophosphate Raman spectrum recorded upon compression between 1 and 3 GPa [16, 18]. The presence of an additional peak near 770  $\text{cm}^{-1}$  indicates that  $\text{P}_2\text{O}_7$  dimers have formed during decompression from 12 GPa.

Pressure alone has little effect on the length of the phosphate chains leading only to minor dimerization. Pressure-induced dimerization was observed in isolated tetrahedra of orthosilicates and orthogermanates [25, 26].

Figure 4 shows a series of Raman spectra recorded at different compression stages of crystalline zinc orthophosphate powder under pressures up to 4 GPa and after decompression, at 120 °C. The same changes than previously can be observed: peaks broaden increase, irreversible structural modification and minor polymerization are observed but at lower pressure.

**Table 1** Overview of the different characteristics of the Raman spectra recorded for the different phosphates before and after mechanical solicitation and for the tribological films (Data extracted from Figs. 1, 2, 3, 4, 5, 6, 7, 8, 9, 10)

	Peak shift ( $\text{cm}^{-1}$ )	Attribution	Relative intensity (a.u.)	FWHM ( $\text{cm}^{-1}$ )	Area (a.u.)	Area (%)
Crystalline zinc orthophosphate	965.5	$\nu_{\text{P-O}}$	2,344.6	14.1	27,236.2	31.8
	1,007.8	$\nu_{\text{P-O}}$	3,144.9	11.5	30,874.1	36.1
	1,045.5	$\nu_{\text{P-O}}$	3,150.6	10.2	27,430.5	24.1
Melted zinc orthophosphate	966.0	$\nu_{\text{P-O}}$	1,111.8	100.0	88,164.6	77.5
	1,070.0	$\nu_{\text{P-O}}$	297.4	100.0	25,661.4	19.4
Zinc orthophosphate after decompression	762.7	$\nu_{\text{P-O-P}}$	126.7	100.0	36,459.2	27.6
	948.3	$\nu_{\text{P-O}}$	272.2	8.3	4,793.9	3.6
	959.7	$\nu_{\text{P-O}}$	366.2	21.5	16,562.1	12.5
	1,004.5	$\nu_{\text{P-O}}$	252.2	100.0	74,270.7	56.2
Zinc orthophosphate after decompression and after cooling	760.8	$\nu_{\text{P-O-P}}$	83.8	100.0	23,914.1	19.1
	955.7	$\nu_{\text{P-O}}$	499.9	25.5	26,126.7	20.8
	1,008.5	$\nu_{\text{P-O}}$	268.7	100.0	75,431.0	60.1
Zinc orthophosphate after tribological test at RT	554.2	$\nu_{\text{Iron oxide}}$	1,742.5	100.0	140,002.0	42.3
	674.9	$\nu_{\text{Iron oxide}}$	207.0	39.3	4,678.1	1.4
	967.0	$\nu_{\text{P-O}}$	2,453.8	89.1	185,975.0	56.2
Zinc orthophosphate after tribological test at 120 °C	552.7	$\nu_{\text{Iron oxide}}$	3,407.0	100.0	272,236.0	39.1
	663.2	$\nu_{\text{Iron oxide}}$	1,123.9	46.9	32,754.0	4.7
	977.3	$\nu_{\text{P-O}}$	4,602.2	100.0	390,608.0	56.2
Crystalline zinc metaphosphate	705.7	$\nu_{\text{P-O-P}}$	31,237.7	11.1	246,431.0	50.0
	1,211.9	$\nu_{\text{P-O}}$	31,185.5	10.5	246,209.0	50.0
Melted zinc metaphosphate	684.0	$\nu_{\text{P-O-P}}$	354.5	100.0	30,285.3	54.2
	1,182.0	$\nu_{\text{P-O}}$	482.0	60.6	25,580.3	45.8
Zinc metaphosphate after decompression	709.0	$\nu_{\text{P-O-P}}$	2,940.2	15.1	133,361.0	35.9
	1,212.0	$\nu_{\text{P-O}}$	3,947.1	19.4	237,802.0	64.1
Zinc metaphosphate after decompression and after cooling	716.0	$\nu_{\text{P-O-P}}$	999.1	45.5	134,546.0	63.0
	1,206.6	$\nu_{\text{P-O}}$	567.8	50.4	79,045.1	37.0
Zinc metaphosphate after tribological test at RT	755.7	$\nu_{\text{P-O-P}}$	285.4	100.0	23,553.8	15.9
	965.9	$\nu_{\text{P-O}}$	424.2	100.0	35,915.7	24.2
	1,070.0	$\nu_{\text{P-O}}$	1,041.0	100.0	89,133.5	60.0
Zinc metaphosphate after tribological test at 120 °C	968.0	$\nu_{\text{P-O}}$	1,994.2	100.0	168,972.0	61.0
	1,080.3	$\nu_{\text{P-O}}$	1,259.3	100.0	108,054.0	39.0
Iron oxide at RT	310.0	$\nu_{\text{magnetite}}$	964.3	100.0	72,174.5	27.8
	542.0	$\nu_{\text{magnetite}}$	850.6	100.0	67,929.1	26.2
	664.0	$\nu_{\text{magnetite}}$	3,135.9	46.9	119,412.0	46.0
Iron oxide at 120 °C	309.0	$\nu_{\text{magnetite}}$	962.8	100.0	72,063.2	27.8
	539.0	$\nu_{\text{magnetite}}$	855.9	100.0	68,350.0	26.3
	668.0	$\nu_{\text{magnetite}}$	3,136.0	47.0	119,121.0	45.9

### 3.2.2 Zinc Metaphosphate

Raman spectra of crystalline zinc metaphosphate were recorded up to 13 GPa and after decompression (Fig. 5). As for the zinc orthophosphate sample, a shift of the peak positions to higher wavenumbers is observed when the pressure increases. All along the compression phase, the two bands are split into several bands, the bandwidth increases, and spectral features are less and less resolved.

We interpret these transformations in the Raman spectra as a distortion of the chains and increase of stress in the sample powder at high pressure. When the pressure is released, those transformations are largely reversed. Peaks in the decompressed sample have similar positions to those of the starting material. The sample is partially disordered as confirmed by enlarged bands in the Raman spectrum of the decompressed sample (about  $13 \text{ cm}^{-1}$  FWHM) when compared with the starting material (about  $9 \text{ cm}^{-1}$

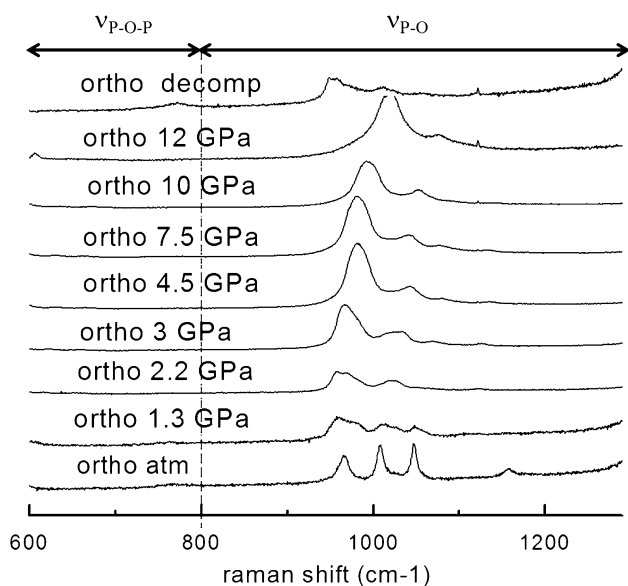


**Fig. 3** In situ Raman spectra of zinc orthophosphate in the 600–1,250  $\text{cm}^{-1}$  range during DAC experiment at room temperature up to 12 GPa of hydrostatic pressure and after effective pressure release

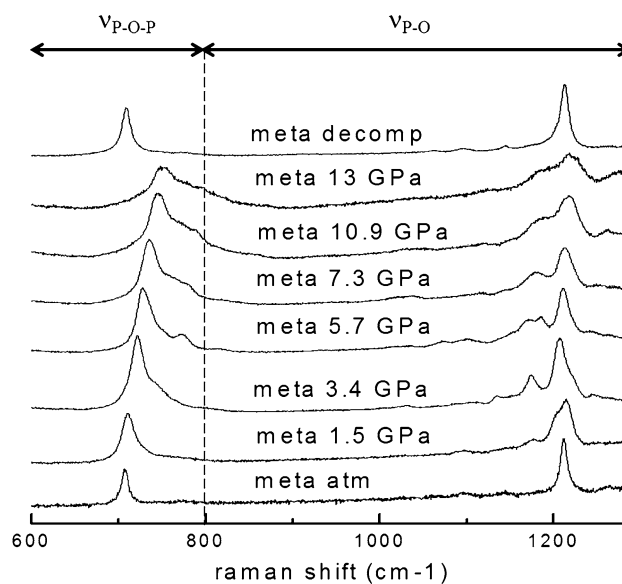


**Fig. 5** In situ Raman spectra of zinc metaphosphate in the 600–1,250  $\text{cm}^{-1}$  range during DAC experiment at room temperature up to 13 GPa of hydrostatic pressure and after effective pressure release

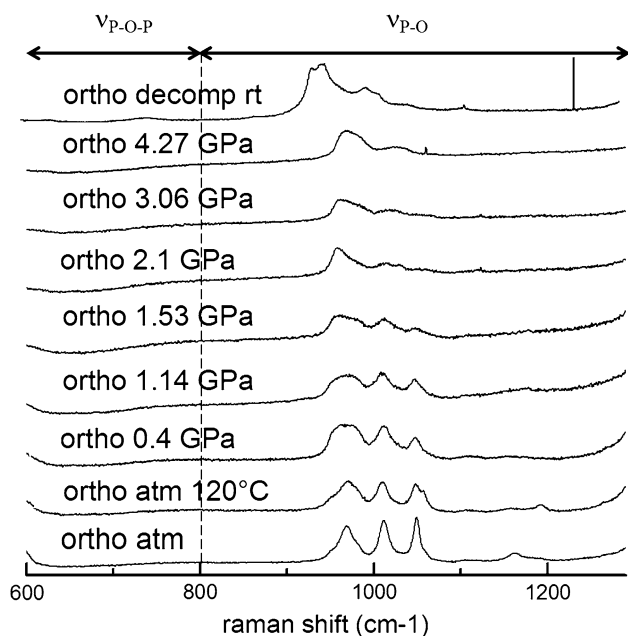


**Fig. 4** In situ Raman spectra of zinc orthophosphate in the 600–1,250  $\text{cm}^{-1}$  range during DAC experiment at 120 °C up to 4 GPa of hydrostatic pressure and after effective pressure release

FWHM). There is no indication of depolymerization of phosphate chains.

Same experiments were done at 120 °C up to 10 GPa and after decompression (Fig. 6). Similar results as those obtained at room temperature have been observed.

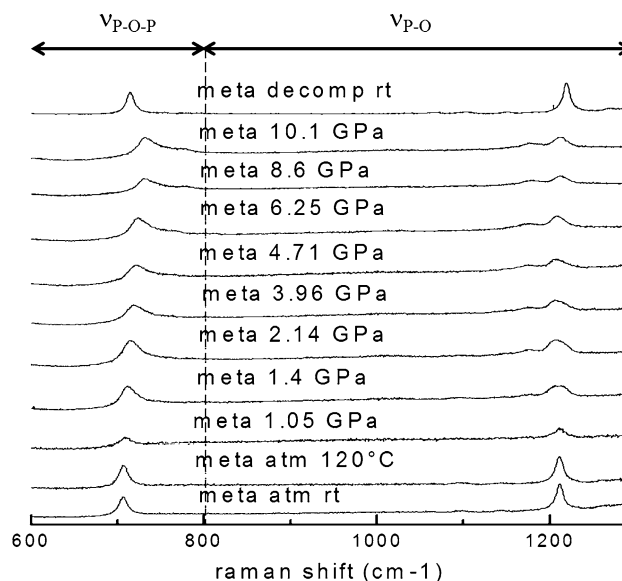


**Fig. 6** In situ Raman spectra of zinc metaphosphate in the 600–1,250  $\text{cm}^{-1}$  range during DAC experiment at 120 °C up to 10 GPa of hydrostatic pressure and after effective pressure release

### 3.3 Behavior of Zinc Polyphosphates Under Tribological Stress

The behavior of the two model materials under tribological stress was investigated both at ambient temperature and at 120 °C. The ability of the materials to form tribofilms was studied and Raman spectroscopy analysis was carried out on the tribo-stressed areas. Test runs with only PAO6 (base oil) were performed in the same conditions.

### 3.3.1 Tribological Behavior with PAO Lubrication Only

Figure 7 shows the Raman spectra recorded on the wear track after a friction test performed at ambient temperature and at 120 °C. Both spectra are characterized by a main peak of strong intensity at  $664\text{ cm}^{-1}$ , and two low-intensity broad bands at around  $310$  and  $542\text{ cm}^{-1}$ . These peak positions are consistent with those of the magnetite [27]. This indicates clearly that the wear track obtained by tribological solicitation in a pure PAO6 lubricated environment is composed essentially of magnetite as a mechanically hard iron oxide.

### 3.3.2 Tribological Behavior of the “PAO + Zinc Orthophosphate” Dispersion

Figure 8 shows the Raman spectra recorded from pure crystalline zinc orthophosphate powder before and after the friction test performed with the “PAO6 +  $\text{Zn}_3(\text{PO}_4)_2$ ” dispersion at ambient temperature and 120 °C. Raman analysis on the wear track evidences the presence of a zinc phosphate tribofilm after the friction tests performed at room temperature and at 120 °C. In both experiments, the spectra have lost the characteristic bands of the crystalline state of the zinc orthophosphate and show a high-intensity broad band at  $967\text{ cm}^{-1}$  (Fig. 8). This indicates a tribo-induced irreversible amorphization of zinc orthophosphate. No band is present in the region of vibrational modes of the P–O–P bonds ( $600\text{--}800\text{ cm}^{-1}$ ), indicating that zinc orthophosphate does not polymerize during the test, even at 120 °C. In addition, two low-intensity broad bands at around  $550$  and  $664\text{ cm}^{-1}$ , absent from the spectrum of zinc orthophosphate,

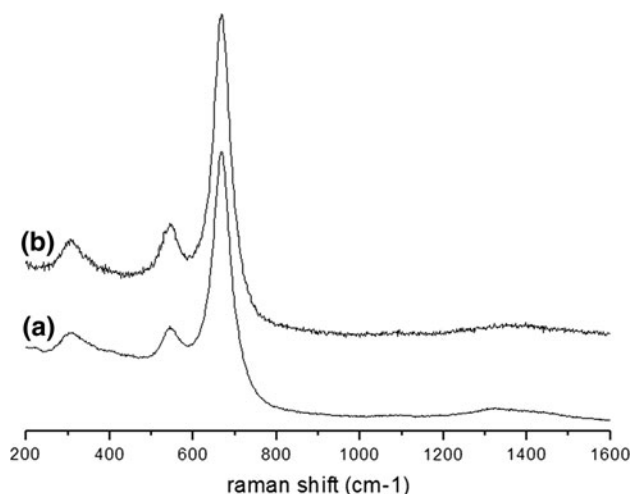


**Fig. 7** Raman spectra in the  $200\text{--}1,600\text{ cm}^{-1}$  range of: **a** tribofilms obtained after a sliding test of steel/steel contact (Hertzian maximum pressure of 1.16 GPa, sliding speed of  $2.5\text{ mm s}^{-1}$ ) lubricated with pure PAO at room temperature and **b** at 120 °C showing typical spectrum of magnetite [27]

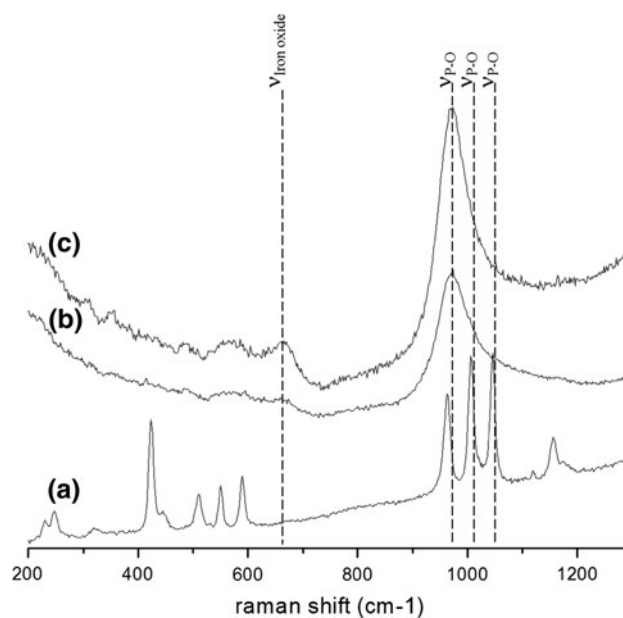
are assigned to the vibrations of magnetite mixed with the tribofilm (Fig. 7).

The main effect of tribological shear and stress on pure zinc crystalline orthophosphate is extensive amorphization, whatever the temperature. Tetrahedra are little distorted in the amorphous tribofilm, even less than in the liquid zinc orthophosphate (Fig. 2a), as indicated by a very weak high-frequency shoulder corresponding to antisymmetric stretching mode of the tetrahedra. No significant polymerization of phosphate is observed in the tribofilm, while partial dimerization was observed after compression–decompression cycle to 12 GPa.

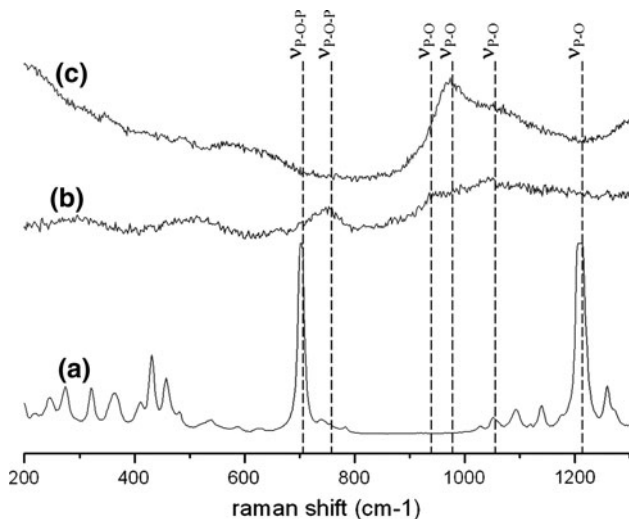
### 3.3.3 Tribological Behavior of the “PAO + Zinc Metaphosphate” Dispersion

Figure 9 shows the Raman spectra recorded from pure crystalline zinc metaphosphate powder  $\text{Zn}(\text{PO}_3)_2$  before friction and on the rubbed surface after the friction test performed with the “PAO6 +  $\text{Zn}(\text{PO}_3)_2$ ” dispersion at ambient temperature and 120 °C.

Raman analysis of the wear track after the tribological test shows clearly the presence of a zinc phosphate-based tribofilm. The tribofilm observed at room temperature is thinner and displays a less intense Raman signal than the one obtained at 120 °C. Thus, we focus first on the spectrum recorded on the tribofilm obtained at 120 °C. It shows a high-intensity broad band at  $968\text{ cm}^{-1}$  and high-frequency



**Fig. 8** Raman spectra in the  $200\text{--}1,600\text{ cm}^{-1}$  range of: **a** pure crystalline orthophosphate ( $\alpha\text{-Zn}_3(\text{PO}_4)_2$ ), **b** tribofilms obtained after a sliding test of steel/steel contact (Hertzian maximum pressure of 1.16 GPa, sliding speed of  $2.5\text{ mm s}^{-1}$ ) lubricated with PAO6 +  $\text{Zn}_3(\text{PO}_4)_2$  at room temperature and **c** at 120 °C



**Fig. 9** Raman spectra in the 200–1,600  $\text{cm}^{-1}$  range of: **a** pure crystalline zinc metaphosphate ( $\beta\text{-Zn}(\text{PO}_3)_2$ ), **b** tribofilms obtained after a sliding test of steel/steel contact (Hertzian maximum pressure of 1.16 GPa, sliding speed of  $2.5 \text{ mm s}^{-1}$ ) lubricated with PAO6 +  $\text{Zn}(\text{PO}_3)_2$  at room temperature and **c** at  $120^\circ\text{C}$

shoulder near  $1,080$  and  $1,150 \text{ cm}^{-1}$  that replace the characteristic peaks of the zinc metaphosphate compound in the  $1,000\text{--}1,200 \text{ cm}^{-1}$  region. This indicates both an amorphization and a depolymerization of the zinc metaphosphate sample. The P–O–P vibration band of the zinc metaphosphate at  $707 \text{ cm}^{-1}$  is no longer observed. A broad peak centered at  $600 \text{ cm}^{-1}$  is observed. This spectrum is very similar to that obtained after a friction test performed with the dispersion “PAO6 + zinc orthophosphate” as shown in Fig. 10. The high-frequency shoulders of the  $968 \text{ cm}^{-1}$  peak are attributed to antisymmetric stretching modes and indicate that tetrahedra are strongly distorted, possible because of a mixed Fe and Zn composition of the tribofilm. The broad peak near  $600 \text{ cm}^{-1}$  could correspond to antisymmetric bending vibrations of the tetrahedra, again consistent with large tetrahedral distortion and possible mixture of Zn and Fe in the film.

The spectrum obtained at ambient temperature is more complex. Broad overlapping bands at  $\approx 940\text{--}1,050\text{--}1,150 \text{ cm}^{-1}$  are observed together with a peak in the region of the P–O–P bond vibrations near  $760 \text{ cm}^{-1}$ . All these peaks occur at similar frequencies to those of phosphate dimers in zinc pyrophosphate [17] that indicates less advanced depolymerization than in the tribofilm obtained at  $120^\circ\text{C}$  where only monomers are observed. Thus, a slight increase in temperature enhances the advancement of depolymerization of the zinc metaphosphate under mechanical stress.

The combined effect of temperature of  $120^\circ\text{C}$ , Hertzian contact pressure of 1.1 GPa and shear, enables a total depolymerization of zinc metaphosphate. The absence of

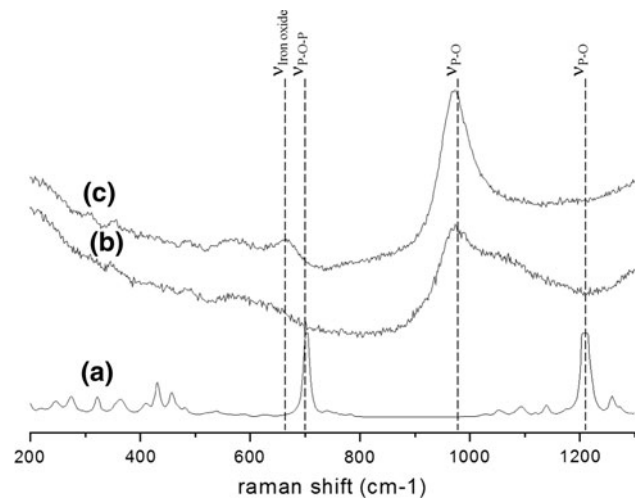


**Fig. 10** Raman spectra in the 200–1,600  $\text{cm}^{-1}$  range of: **a** pure crystalline zinc metaphosphate ( $\beta\text{-Zn}(\text{PO}_3)_2$ ), **b** tribofilms obtained after a sliding test of steel/steel contact (Hertzian maximum pressure of 1.16 GPa, sliding speed of  $2.5 \text{ mm s}^{-1}$ ) at  $120^\circ\text{C}$  lubricated with PAO6 +  $\text{Zn}(\text{PO}_3)_2$  and **c** lubricated with PAO6 +  $\text{Zn}_3(\text{PO}_4)_2$

typical signal from iron oxides may be correlated with incorporation of Fe in the phosphate tribofilm.

Table 1 gives an overview of the different characteristics of the Raman spectra (peak Raman shift, relative peak intensity and FMHW) recorded from the different phosphates before and after mechanical stress and from the tribological films (Figs. 1, 2, 3, 4, 5, 6, 7, 8, 9, 10).

#### 4 Discussion

Zinc polyphosphate compounds (orthophosphate and metaphosphate composition) were mechanically stressed under different conditions of pressure, shear and temperature. It was shown in this study that the pressure alone, up to 13 GPa, induces only a partial amorphization (or loss of crystallinity, grain size reduction...) of both the zinc ortho- and metaphosphate. An irreversible transformation is observed in the orthophosphate sample after decompression, while high-pressure transformations of the metaphosphate sample are essentially reversible.

The results obtained on zinc orthophosphates are consistent with those already obtained by Gauvin et al. [16] and Shakhvorostav et al. [18]. In addition, a minor polymerization of zinc orthophosphate, marked by the appearance of phosphate dimer Raman bands in the decompressed sample spectrum, could be observed in the sample decompressed from 12 GPa. It is unlikely that the modest pressures of about 1 GPa generated in tribological contacts can induce significant polymerization. Thus, our experiments demonstrate that pressure induces only structural disordering of zinc polyphosphates. This result do not support Nicholls’ theory [2],



suggesting that pressure alone could play an important role in the formation of the phosphate chains gradient, especially in view of the major role of the large stress and shear in a tribological contact.

The tribological tests on zinc polyphosphates showed clearly that both shear and temperature have a strong influence on the ability of these compounds to form adherent tribofilms. Analyses performed on the wear scars after tribological tests performed at room temperature with zinc polyphosphates (ortho and meta) demonstrate extensive amorphization of these compounds, marked by the extremely broad Raman bands. These results are in agreement with those obtained by Gauvin et al. [17] in a previous study of orthophosphates. Here, a depolymerization of zinc metaphosphate was evidenced during the formation of antiwear tribofilm. Depolymerization is partial at ambient temperature, leading to formation of pyrophosphate film, and much more advanced at 120 °C with formation of a pure orthophosphate film. The presence of iron oxide in the tribofilm is unambiguously observed only when orthophosphate is used as a starting material. Iron oxide particles were not observed in the tribofilms obtained from the metaphosphates, suggesting that mixed amorphous Fe- and Zn-phosphates are formed during depolymerization of the metaphosphate.

These results complement the observations of Crobu et al. [20], who performed tribological tests by rubbing steel balls against a zinc metaphosphate disks in a poly- $\alpha$ -olefin bath at room temperature. The tribostressed areas on both metaphosphate disks and steel balls were characterized. The authors used XPS to demonstrate the presence of shorter phosphate chains inside the tribo-tracks on the disks. Moreover, iron was transferred to the glass during the tribological tests. Here, the tribochemical reaction between zinc metaphosphate and iron leads to depolymerization and the formation of mixed zinc-iron phosphate in the tribofilm at 120 °C even when an ordered crystalline phosphate is used.

Tribochemical reactions between zinc metaphosphate and iron oxide species present at the surface of the steel substrate have been proposed by Martin [12]. Based on the chemical hardness model developed by Pearson [13], zinc metaphosphate would react with iron oxides to form a mixed zinc and iron phosphate glass. This reaction leads to a depolymerization of the polyphosphate chain near the substrate and can well explain the phosphate chains gradient observed in the tribofilm by XPS and its composition made of mixed Fe/Zn polyphosphates. Moreover, this model was recently supported by computational works [28, 29]. Molecular Dynamics and quantum chemistry was used to simulate the reaction between iron oxide particles and zinc polyphosphate glass. It was shown that the combined effect of pressure and shear is necessary for the reaction to

occur in the tribological contact and that the pressure alone is not sufficient to initiate the reaction. It was also shown that at 1 GPa contact pressure, the reaction starts even at low sliding speeds ( $0.1 \text{ ms}^{-1}$ ) at 353 K. In the absence of shear, these authors found that at atmospheric pressure, the reaction between zinc metaphosphate and iron oxide nanoparticles is possible only at elevated temperature (1,700 K), where diffusion is efficient. The experimental results obtained here are in good agreement with the theoretical ones. The energy barrier necessary for the depolymerization of the zinc metaphosphate is overcome when combining pressure, shearing and modest temperature (120 °C or 393 K). It is likely that shearing provides an alternative to diffusion by promoting direct mechanical transport and mixing at the scale of the tribofilm ( $\approx 100 \text{ nm}$ ). However, as far as no high-pressure experiment was done in presence of iron oxide particles, it is difficult to conclude on the exact role of the shear stress on the results obtained in this work. Such experiments (in presence of different iron oxide species— $\text{Fe}_2\text{O}_3$ ,  $\text{Fe}_3\text{O}_4$ ,  $\text{FeO}$  ...) will be performed in a near future, both at ambient temperature and 120 °C. The objectives will be to probe the possible solid state chemical reactions between zinc metaphosphates and iron oxides in the absence of shear stress. In addition, new tribological tests will be performed in the same experimental conditions than those reported in this work but with a much less reactive substrate than steel. Thus, the role of the shear stress will be investigated without considering the influence of the iron oxide. The role of these two parameters will thus be much more precisely investigated.

## 5 Conclusion

The effects of pressure, shear and temperature on the structure of zinc polyphosphate compounds were investigated using *ex situ* Raman spectroscopy of tribofilms synthesized from zinc phosphates and *in situ* Raman spectroscopy performed in the DAC. The following results have been obtained:

- On zinc phosphates, pressure alone (at room temperature) induces either reversible (meta) or irreversible (ortho) structural disorder, but does not affect significantly the chain length in the phosphate samples. Minor polymerization has only been observed for zinc orthophosphate.
- Tribological tests performed at room temperature and 120 °C with dispersions of zinc polyphosphates in base oil lead to the formation of adherent tribofilms on the steel surface. An amorphous-zinc-orthophosphate-based tribofilm mixed with iron oxides is obtained with

$\alpha$ -Zn<sub>3</sub>(PO<sub>4</sub>)<sub>2</sub>, while an amorphous tribofilm made of either partially or fully depolymerized zinc metaphosphate is obtained at ambient and high temperature, respectively.

- It can be concluded that shear is needed to observe a depolymerization of the zinc metaphosphate and that temperature (120 °C) speeds up this depolymerization.
- Depolymerization of the zinc metaphosphate in presence of iron under tribological conditions can be explained by a tribochemical reaction between the polyphosphates and iron oxides of the steel substrate.

**Acknowledgments** The authors would like to thank the “Région Rhone-Alpes” for financial support through the “ARC Energies”. The Raman facility at ENS Lyon is supported by the Institut National des Sciences de l’Univers (INSU).

## References

1. Aktary, M., McDermott, M.T., McAlpine, G.A.: Morphology and nanomechanical properties of ZDDP antiwear films as a function of tribological contact time. *Tribol. Lett.* **12**, 155–162 (2002)
2. Nicholls, M.A., Bancroft, G.M., Norton, P.R., Kasrai, M., Stasio, G.D., Frazer, B.H., Wiesec, L.M.: Nanometer scale chemomechanical characterization of antiwear films. *Tribol. Lett.* **17**, 245–259 (2004)
3. Spikes, H.: The history and mechanisms of ZDDP. *Tribol. Lett.* **17**, 469–489 (2004)
4. Nicholls, M.A., Do, T., Norton, P.R., Kasrai, M., Bancroft, G.M.: Review of the lubrication of metallic surfaces by zinc dialkyl dithiophosphates. *Tribol. Int.* **38**, 15–39 (2005)
5. Willermet, P.A., Dailey, D.P., Carter, R.O., Schmitz, P.J., Zhu, W.: Mechanism of formation of antiwear films from zinc dialkyl dithiophosphates. *Tribol. Int.* **28**, 177–187 (1995)
6. Fuller, M.L.S., Kasrai, M., Bancroft, G.M., Fyfe, K., Tan, K.H.: Solution decomposition of zinc dialkyl dithiophosphate and its effect on antiwear and thermal film formation studied by X-ray absorption spectroscopy. *Tribol. Int.* **31**, 627–644 (1998)
7. Armstrong, D.R., Ferrari, E.S., Roberts, K.J., Adams, D.: An examination of the reactivity of zinc di-alkyl-di-thiophosphate in relation to its use as an anti-wear and anti-corrosion additive in lubricating oils. *Wear* **217**, 276–287 (1998)
8. Bovington, C.H., Dacre, B.: The adsorption and reaction of decomposition products of zinc di-isopropyldiophosphate on steel. *ASLE Trans.* **27**, 252–258 (1983)
9. Dickert, J.J., Rowe, C.N.: Thermal decomposition of metal O, O-dialkylphosphorodithioates. *J. Org. Chem.* **32**, 647–653 (1967)
10. Fuller, M., Yin, Z., Kasrai, M., Bancroft, G.M., Yamaguchi, E.S., Ryason, P.R., Willermet, P.A., Tan, K.H.: Chemical characterization of tribochemical and thermal films generated from neutral and basis ZDDPs using X-Ray absorption spectroscopy. *Tribol. Int.* **30**, 305–315 (1997)
11. Yin, Z., Kasrai, M., Fuller, M., Bancroft, G.M., Fyfe, K., Tan, K.H.: Application of soft X-ray absorption spectroscopy in chemical characterization of antiwear films generated by ZDDP Part I: the effects of physical parameters. *Wear* **202**, 172–191 (1997)
12. Martin, J.M.: Antiwear mechanisms of zinc dithiophosphate: a chemical hardness approach. *Tribol. Lett.* **6**, 1–8 (1999)
13. Pearson, R.G.: *Chemical Hardness*. Wiley, New York (1997)
14. Mosey, N.J., Woo, T.K., Kasrai, M., Norton, P.R., Bancroft, G.M.: Interpretation of experiments on ZDDP anti-wear films through pressure-induced cross-linking. *Tribol. Lett.* **24**, 105–114 (2006)
15. Gauvin, M. Ph.D. thesis, Ecole Centrale de Lyon, Ecully (2008)
16. Gauvin, M., Dassenoy, F., Minfray, C., Martin, J.M., Montagnac, G., Reynard, B.: Zinc phosphate chain length study under high hydrostatic pressure by Raman spectroscopy. *J. Appl. Phys.* **101**, 063505–063513 (2007)
17. Gauvin, M., Dassenoy, F., Belin, M., Minfray, C., Guerret-Piecourt, C., Bec, S., Martin, J.M., Montagnac, G., Reynard, B.: Boundary lubrication by pure crystalline zinc orthophosphate. *Tribol. Lett.* **31**, 139–148 (2008)
18. Shakhvorostov, D., Müser, M.H., Mosey, N.J., Munoz-Paniagua, D.J., Pereira, G., Song, Y., Kasrai, M., Norton, P.R.: On the pressure-induced loss of crystallinity in orthophosphates of zinc and calcium. *J. Chem. Phys.* **128**, 074706–074710 (2008)
19. Shakhvorostov, D., Müser, M.H., Mosey, N.J.: Correlating cation coordination, stiffness, phase transition pressures, and smart materials behavior in metal phosphates. *Phys. Rev. B* **79**, 094107–094112 (2009)
20. Crobu, M., Rossi, A., Mangolini, F., Spencer, N.D.: Tribocchemistry of bulk zinc metaphosphate glasses. *Tribol. Lett.* **39**, 121–134 (2010)
21. Crobu, M., Rossi, A., Mangolini, F., Spencer, N.D.: Chain-length-identification strategy in zinc polyphosphate glasses by means of XPS and ToF-SIMS. *Anal. Bioanal. Chem.* **403**, 1415–1432 (2012)
22. Mao, H.K., Xu, J., Bell, P.M.: Calibration of the ruby pressure gauge to 800 kbar under quasi-hydrostatic conditions. *J. Geophys. Res.* **91**, 4673–4676 (1991)
23. Frost, R.L.: An infrared and Raman spectroscopic study of natural zinc phosphates. *Spectrochim. Acta, Part A* **60**, 1439–1445 (2004)
24. Meyer, K.: Characterization of the structure of binary zinc ultraphosphate glasses by infrared and Raman spectroscopy. *J. Non-Cryst. Solids* **209**, 227–239 (1997)
25. Durben, D.J., McMillan, P.F., Wolf, G.H.: Raman study of the high-pressure behavior of forsterite (Mg<sub>2</sub>SiO<sub>4</sub>) crystal and glass. *Am. Miner.* **78**, 1143–1148 (1993)
26. Reynard, B., Petit, P.E., Guyot, F., Gillet, P.: Pressure-induced structural modifications in Mg<sub>2</sub>GeO<sub>4</sub>-olivine: a Raman spectroscopic study. *Phys. Chem. Minerals* **20**, 556–562 (1994)
27. De Faria, D.L.A., Venâncio Silva, S., De Oliveira, M.T.: Raman microspectroscopy of some iron oxides and oxyhydroxides. *J. Raman Spectrosc.* **28**, 873–878 (1997)
28. Onodera, T., Martin, J.M., Minfray, C., Dassenoy, F., Miyamoto, A.: Antiwear chemistry of ZDDP: coupling classical MD and tight-binding quantum chemical MD methods (TB-QCMD). *Tribol. Lett.* **50**, 31–39 (2013)
29. Onodera, T., Morita, Y., Suzuki, A., Sahnoun, R., Koyama, M., Tsuboi, H., Hatakeyama, N., Endou, A., Takaba, H., Kubo, M., Del Carpio, C.A., Minfray, C., Martin, J.M., Miyamoto, A.: A theoretical investigation on the abrasive wear prevention mechanism of ZDDP and ZP tribofilms. *Appl. Surf. Sci.* **254**, 7976–7979 (2008)